Journal of Fluids and Structures 17 (2003) 927–939

JOURNAL OF FLUIDS AND STRUCTURES

www.elsevier.nl/locate/jnlabr/yjfls

Linear vibration analysis of cantilever plates partially submerged in fluid

A. Ergin*, B. Uğurlu

Faculty of Naval Architecture and Ocean Engineering, Istanbul Technical University, Maslak, 80626, Istanbul, Turkey

Received 12 March 2002; accepted 19 March 2003

Abstract

Dynamic characteristics, such as natural frequencies and mode shapes, of cantilever plates, partially in contact with a fluid, are investigated. In the analysis of the linear fluid–structure system, it is assumed that the fluid is ideal, and fluid forces are associated with inertial effects of the surrounding fluid. This implies that the fluid pressure on the wetted surface of the structure is in phase with the structural acceleration. Furthermore, the infinite frequency limit is assumed on the free surface. The in vacuo dynamic properties of the plates are obtained by use of a standard finite-element software. In the *wet* part of the analysis, it is assumed that the plate structure preserves its in vacuo mode shapes when in contact with the surrounding fluid and that each mode shape gives rise to a corresponding surface pressure distribution of the cantilever plate. The fluid–structure interaction effects are calculated in terms of the generalized added-mass values independent of frequency (i.e., infinite frequency generalized added-masses), by use of a boundary-integral equation method together with the method of images in order to impose the $\Phi = 0$ boundary condition on the free surface. To assess the influence of the surrounding fluid on the dynamic characteristics, the wet natural frequencies and associated mode shapes were calculated, and they compared very well with the available experimental data and numerical predictions.

1. Introduction

An accurate understanding of the dynamic interaction between an elastic structure and fluid is necessary in various engineering problems. Examples include vibration of floating structures (ships, offshore platforms, etc.) excited by wave impact, water-retaining structures (dams, storage vessels, etc.) under earthquake loading, etc. The local resonant vibration behavior of individual plates has also been a great concern to the shipbuilder and operator for many years. Therefore, considerable effort has been made in the study of the vibrational response of plates, partially or totally immersed in the fluid.

Lindholm et al. (1965) experimentally investigated the resonance frequencies of cantilever plates in air, totally or partially immersed in water, and compared the measurements with the theoretical predictions. They evaluated the fluid actions using a strip-theory approach. Meyerhoff (1970) calculated the added mass of thin rectangular plates in infinite fluid, and described the potential flow around a flat rectangular plate by use of dipole singularities. The finite-element method has also been applied to solve the fluid–structure interaction problems for completely submerged elastic plates (see, for example, Muthuveerappan et al., 1979; Rao et al., 1993). On the other hand, Fu and Price (1987) studied the dynamic behavior of a vertical or horizontal cantilever plate totally or partially immersed in fluid. In their analysis, they calculated the generalized fluid loading to assess the influences of free surface and submerged plate length on the

*Corresponding author. Tel.: +90-212-285-6414; fax: +90-212-285-6454.
E-mail address: ergina@itu.edu.tr (A. Ergin).

0889-9746/03/$ - see front matter
doi:10.1016/S0889-9746(03)00050-1

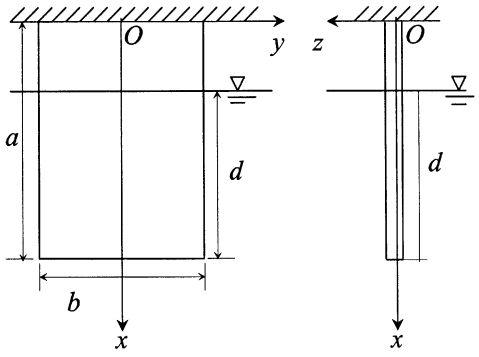

Fig. 1. Cantilever plate partially submerged in fluid.

dynamic characteristics. Recently, Liang et al. (2001) adopted an empirical added-mass formulation to determine the frequencies and mode shapes of submerged cantilever plates, and compared their results with the available experimental data and numerical predictions.

In this work, the dynamic characteristics (i.e., wet natural frequencies and mode shapes) of vibrating cantilever plates, partially or totally immersed within the fluid, as illustrated in Fig. 1, are studied, assuming a linear fluid–structure system. In this investigation, it is assumed that the fluid is ideal, i.e., inviscid and incompressible, and its motion is irrotational. Furthermore, the fluid forces are associated with the inertial effect of the fluid. This means that the fluid pressure on the wetted surface of the structure is in phase with the acceleration. In the analysis, it is assumed that the *dry* plate vibrates in its in vacuo eigenmodes when it is in contact with fluid, and that each mode gives rise to a corresponding surface pressure distribution on the wetted part of the structure. The in vacuo dynamic analysis entails the vibration of the cantilever plate in the absence of any external force and structural damping, and the corresponding dynamic characteristics (e.g., natural frequencies and principal mode shapes) of the plate structure were obtained using ANSYS, a standard finite-element software.

At the fluid–structure interface, the body-boundary condition requires that the normal velocity of the fluid be equal to that of the structure. The normal velocities on the wetted surface are expressed in terms of the modal structural displacements, obtained from the in vacuo dynamic analysis. By use of a boundary-integral equation method in conjunction with the method of images (i.e., imposing infinite frequency limit condition on the free surface), the fluid pressure is eliminated from the problem and the fluid–structure interaction forces are calculated solely in terms of the generalized added-mass coefficients that are independent of the vibrational frequency. As a result of the boundary condition imposed on the free surface, the hydrodynamic damping becomes zero.

In this analysis, the wet surface is idealized by use of appropriate boundary elements, referred to as hydrodynamic panels. The generalized structural mass matrix is merged with the generalized added-mass matrix and then the total generalized mass matrix is used in solving the eigenvalue problem for the partially or totally immersed cantilever plate. To assess the influence of the surrounding fluid on the dynamic behavior of the plate structure, wet natural frequencies and associated mode shapes are calculated.

Comparison of the predicted dynamic characteristics with available experimental measurements (Lindholm et al., 1965) and numerical calculations (Fu and Price, 1987) shows very good agreement. Furthermore, the influences of various effects such as the submergence depth, plate aspect ratio (a/b) and thickness ratio (t/b) on the dynamic behavior are also investigated.

2. Mathematical model

2.1. Formulation of the fluid problem

A right-handed Cartesian coordinate system, xyz, is adopted in the present study and it is shown in Fig. 1 for the cantilever plate partially submerged. The coordinate system is fixed in space with its origin at O, and the x- and y-axis coincide with the center-lines of the plate in the longitudinal and transverse directions, respectively. Meanwhile, the z-axis lies across the plate thickness, and it is normal to the x–y plane.

Assuming an ideal fluid and irrotational motion, there exists a fluid velocity vector, **v**, defined as the gradient of the velocity potential function Φ, where Φ satisfies Laplace's equation throughout the fluid domain.

Before describing the responses of the flexible structure, it is necessary to assign coordinates to deflections at various degrees of freedom. One particular set of generalized coordinates having significant advantage is the principal coordinates of the dry structure (see, for example, Bishop et al., 1986; Ergin et al., 1992; Ergin, 1997a). For a structure vibrating in an ideal fluid, with frequency ω, the principal coordinate, describing the response of the structure in the rth modal vibration, may be expressed by

$$p_r(t) = p_r e^{i\omega t}. \tag{1}$$

Therefore, the velocity potential function due to the distortion of the structure in the rth modal vibration may be written as (see, e.g., Ergin and Temarel, 2002; Amabili et al., 1998)

$$\Phi_r(x, y, z, t) = i\omega\phi_r(x, y, z)p_r e^{i\omega t}, r = 1, 2, ..., M, \tag{2}$$

where M represents the number of modes of interest.

On the wetted surface of the vibrating plate, the fluid normal velocity must be equal to the normal velocity of the structure, and this condition for the rth modal vibration can be expressed as

$$-\frac{\partial\phi_r}{\partial n} = \mathbf{u}_r.\mathbf{n}, \tag{3}$$

where $\mathbf{u}_r$ is the rth modal displacement vector of the median surface of the structure and **n** is the unit normal vector on the wetted surface and it points into the fluid.

In this study, it is assumed that the plate structure vibrates at relatively high frequencies so that the effect of surface waves can be neglected. Therefore, the free surface condition (infinite frequency limit condition) for ϕ_r can be approximated by

$$\phi_r = 0, \text{on the free surface.} \tag{4}$$

The method of images (see, e.g., Kito, 1970; Ergin and Temarel, 2002) may be used, as shown in Fig. 2, to satisfy this condition. By adding an imaginary boundary region, the condition given by Eq. (4) at the horizontal surface can be omitted; thus the problem is reduced to a classical Neumann problem.

By use of Euler's integral and neglecting the higher-order terms, the dynamic fluid pressure on the mean wetted-surface of the flexible plate due to the rth modal vibration becomes

$$P_r(x, y, z, t) = -\rho\frac{\partial\Phi_r}{\partial t}. \tag{5}$$

Substituting Eq. (2) into Eq. (5), the following expression for the pressure is obtained:

$$P_r(x, y, z, t) = \rho\omega^2\phi_r(x, y, z)p_r e^{i\omega t}. \tag{6}$$

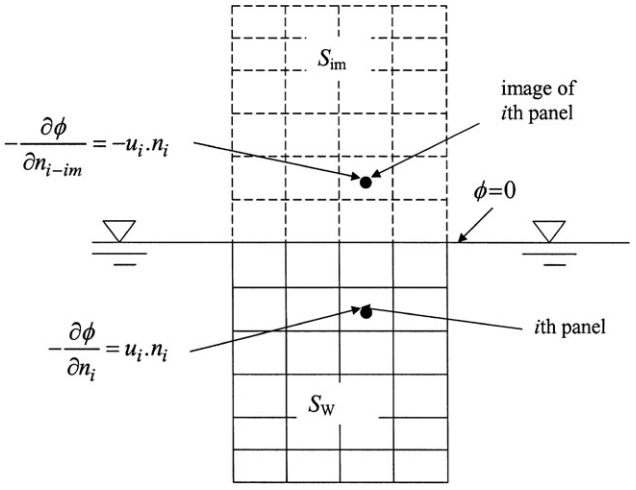

Fig. 2. Wetted and imaginary surfaces for partially submerged plate.

The kth component of the generalized fluid–structure interaction force due to the rth modal vibration of the plate can be expressed in terms of the pressure acting on the wetted surface of the plate as

$$Z_{kr}(t) = \int\int_{S_w} P_r \mathbf{u}_k \mathbf{n}\, \mathrm{d}S = p_r \mathrm{e}^{i\omega t} \int\int_{S_w} \rho\omega^2 \phi_r \mathbf{u}_k \mathbf{n}\, \mathrm{d}S. \tag{7}$$

The generalized added-mass term A_{kr} can be defined as

$$A_{kr} = \rho \int\int_{S_w} \phi_r \mathbf{u}_k \mathbf{n}\, \mathrm{d}S. \tag{8}$$

Therefore, the generalized fluid–structure interaction force component, Z_{kr}, can be rewritten as

$$Z_{kr}(t) = A_{kr}\omega^2 p_r \mathrm{e}^{\mathrm{i}\omega t} = -A_{kr}\ddot{p}_r(t). \tag{9}$$

It should be noted, as a result of the infinite frequency limit condition imposed on the free surface, that the generalized added-mass coefficients are constants and are independent of the vibrational frequency, and that the hydrodynamic damping is zero.

2.2. Numerical evaluation of deformation potential ϕ

The deformation potential, ϕ, in a three-dimensional inviscid flow field due to the oscillating elastic structure can be expressed by means of a distribution of unknown source strengths, σ, over the wetted and imaginary surfaces of the structure (see, e.g., Hess and Smith, 1967; Hess, 1975) in the following form:

$$\phi(\mathbf{r}) = \int\int_{S_w+S_{im}} \frac{\sigma(\mathbf{r}_0)}{R(\mathbf{r},\mathbf{r}_0)} \mathrm{d}S, \tag{10}$$

where

$$R = \left[(x-x_0)^2+(y-y_0)^2+(z-z_0)^2\right]^{\frac{1}{2}}$$

and $\mathbf{r} = (x,y,z)$ denotes the position vector of the field point within the fluid, $\mathbf{r}_0 = (x_0, y_0, z_0)$ is the position vector of the source points on the wetted or image surface of the plate.

Substituting the boundary condition (3) into Eq. (10), the distribution of the unknown strengths σ_i can be determined from the set of following algebraic equations:

$$2\pi\sigma_i - \sum_{j=1}^{N} \sigma_j \int\int_{\Delta S_j} \frac{\partial}{\partial n}\left[\frac{1}{R(\mathbf{r}_j,\mathbf{r}_j)}\right] \mathrm{d}S = u_{ni}, \quad i = 1,2,...,N, \tag{11}$$

where ΔS_j represents the area of the jth panel, N is the number of panels used to discretize the wetted and imaginary surfaces and u_{ni} denotes the modal displacement in the direction of the normal at the control point (x_i, y_i, z_i) of the ith panel.

2.3. Calculation of wet frequencies and mode shapes

It should be remembered that when a body oscillates in an unbounded, inviscid fluid, the generalized added-mass coefficients are constants, independent of frequency, and the generalized fluid damping coefficients are zero. However, in the case when the body oscillates in or near a free surface, the hydrodynamic coefficients exhibit frequency dependence in the low-frequency region, but show a tendency towards a constant value in the high-frequency region. In this study, it is assumed that the structure vibrates in the high-frequency region so that the generalized added-mass values are constants and evaluated by use of Eq. (8). Furthermore, the generalized hydrodynamic damping and fluid stiffness are assumed to be zero. Hence, the generalized equation of motion for the dynamic fluid–structure interaction system (see, e.g., Ergin, 1997b, c), assuming free vibrations with no structural damping, is

$$\left[-\omega^2(\mathbf{a}+\mathbf{A})+\mathbf{c}\right]\mathbf{p} = \mathbf{0} \tag{12}$$

where $\mathbf{a}$ and $\mathbf{c}$ denote the generalized structural mass and stiffness matrices, respectively. The matrix $\mathbf{A}$ represents the infinite frequency generalized added-mass coefficients.

Solving the eigenvalue problem, expressed by Eq. (12), yields the wet frequencies and associated mode shapes of the cantilever plate in contact with the fluid. To each wet frequency ω_r, there is a corresponding wet eigenvector $\mathbf{p}_{\mathrm{or}} = \{p_{r1}, p_{r2,...,}p_{rm}\}$ satisfying Eq. (12). The corresponding uncoupled wet mode shapes for the structure partially or totally in

contact with fluid are obtained as

$$\bar{\mathbf{u}}_r(x,y,z) = \{\bar{u}_r, \bar{v}_r, \bar{w}_r\} = \sum_{j=1}^{M} \mathbf{u}_j(x,y,z)\mathbf{p}_{rj}, \tag{13}$$

where $\mathbf{u}_j(x,y,z) = \{u_j, v_j, w_j\}$ denote the in vacuo mode shapes of the *dry* cantilever plate and M the number of mode shapes included in the analysis. It should be noted that the fluid–structure interaction forces associated with the inertial effect of the fluid do not have the same spatial distribution as those of the in vacuo modal forms. Consequently, this produces hydrodynamic coupling between the in vacuo modes. This coupling effect is introduced into Eq. (12) through the generalized added-mass matrix **A**.

3. Numerical results and comparisons

A series of calculations have been performed in order to demonstrate the applicability of the aforementioned theory to vibrating cantilever plates, partially or totally immersed within the fluid. Two cantilever plates with different aspect and thickness ratios were considered. The first plate chosen has length $a = 1016$ mm, width $b = 203.2$ mm, thickness $t = 4.84$ mm (see Fig. 1), and it was experimentally studied by Lindholm et al. (1965). The second plate adopted in the present calculations is 10 m long, 10 m wide, 0.238 m thick, and it was numerically investigated by Fu and Price (1987) by use of a three-dimensional hydroelasticity theory. Both plates are made of steel and have the following material characteristics: Young's modulus = 206.8 GPa, Poisson's ratio = 0.3, and mass density = 7830 kg/m^3. Fresh water is used as the surrounding fluid with a density of 1000 kg/m^3.

3.1. Idealization and convergence

The in vacuo dynamic characteristics of cantilever plates were obtained by use of ANSYS (1994), a finite-element software. This produces information on the natural frequencies and principal mode shapes of the *dry* structure. In these calculations, the plates were discretized by four-noded, quadrilateral shell elements, including both membrane and bending stiffness influences.

In a preliminary calculation, 128 elements were distributed over the cantilever plate of Lindholm et al. (1965). The distribution over the plate consists of 16 and 8 equally spaced elements, respectively, along the length and width of the plate structure. To test the convergence of the calculated dynamic properties (natural frequencies and principal mode shapes), the number of elements over the cantilever plate was increased first to 288 (24 elements along the length and 12 elements along the width of the plate) and then to 512 (32 elements along the length and 16 elements along the width of the cantilever). Table 1 shows the experimental results of Lindholm et al. (1965) and calculated natural frequencies obtained from ANSYS, for the first six modes. The differences in the results indicate that the calculated values are converging with increasing number of elements. The results of the final idealization (512 elements) compare very well with the experimental measurements of Lindholm et al. (1965); hence they were adopted for the in vacuo dynamic properties of the cantilever plate. It should be noted that the mode shapes are divided into two distinct groups: the symmetric (S) (bending) and antisymmetric (A) (torsional) distortional mode shapes. A symmetric mode shape shows similar displacement characteristics on either side of the Ox-axis (see Fig. 1), and, on the other hand, an antisymmetric mode shape exhibits opposite displacement behavior about the Ox-axis.

Another series of calculations were performed in order to test the convergence of the hydrodynamic properties (generalized added-mass terms). The aim of this exercise was to represent accurately the distortional mode shapes of the

Table 1
Convergence of FEM (in vacuo) natural frequencies (Hz)

Mode	Mode type	128 elements	288 elements	512 elements	Experiment(Lindholm et al.,1965)
1	S	3.94	3.94	3.94	3.84
2	S	24.65	24.66	24.66	24.20
3	A	38.70	38.99	39.07	39.10
4	S	69.42	69.28	69.24	68.10
5	A	118.17	119.17	119.47	121.00
6	S	136.49	136.64	136.35	—

Table 2
Convergence of wet natural frequencies (Hz)

Mode	Mode type	Depth ratio (d/a)											
		0.25			0.5			0.75			1		
		96 Panels	192 Panels	320 Panels	176 Panels	360 Panels	608 Panels	256 Panels	528 Panels	896 Panels	336 Panels	696 Panels	1184 Panels
1	S	2.21	2.26	2.29	1.85	1.89	1.90	1.78	1.81	1.83	1.78	1.81	1.82
2	S	21.07	21.23	21.32	15.29	15.56	15.69	11.99	12.13	12.20	11.51	11.62	11.68
3	A	28.56	29.17	29.42	24.72	25.23	25.43	23.52	23.98	24.16	23.37	23.83	24.00
4	S	58.63	59.01	59.32	52.16	52.13	52.23	38.39	38.52	38.67	34.35	34.28	34.31
5	A	103.42	104.57	105.01	91.41	93.08	93.84	75.28	76.70	77.31	72.96	73.40	73.91
6	S	117.97	116.84	116.66	100.11	98.91	98.71	85.49	84.55	84.46	72.19	71.58	71.22

Table 3
Comparisons of dry and wet natural frequencies (Hz)

Mode	Mode type	This study					Experiment (Lindholm et al. 1965)				
		In vacuo	Depth ratio (d/a)				In -air	Depth ratio (d/a)			
			0.25	0.5	0.75	1		0.25	0.5	0.75	1
1	S	3.94	2.29	1.90	1.83	1.82	3.84	2.17	1.82	1.79	1.78
2	S	24.66	21.32	15.69	12.20	11.68	24.20	21.01	15.5	11.99	11.50
3	A	39.07	29.42	25.43	24.16	24.00	39.10	29.75	25.50	24.20	24.20
4	S	69.24	59.32	52.23	38.67	34.31	68.10	57.36	51.61	38.27	33.50
5	A	119.47	105.01	93.84	77.31	73.91	121.00	106.35	95.99	79.00	75.26
6	S	136.35	116.64	98.71	84.46	71.22	—	—	—	—	—

wetted surface of the cantilever plate. For the plate of Lindholm et al. (1965), the tests were carried out separately for four different depth ratios, namely $d/a = 0.25$, 0.5, 0.75 and 1. A test case may simply be identified by the number of hydrodynamic panels distributed along the length (NPL) and along the width of the wetted plate. However, the hydrodynamic panels are distributed over the wetted top and bottom plate surfaces separated by the thickness of the plate and over the wetted edge surfaces parallel to the x–z or y–z planes (see Fig. 1). In the first group of idealizations, 96 ($NPL = 4$), 176 ($NPL = 8$), 256 ($NPL = 12$) and 336 ($NPL = 16$) quadratic hydrodynamic panels (boundary elements) were distributed over the wetted surfaces of the cantilever plate, respectively, for the depth ratios $d/a = 0.25$, 0.5, 0.75 and 1. The number of panels along the width of the wetted plate was eight in the first group of idealizations. Subsequently, the number of panels over the wetted surfaces was increased to 192 ($NPL = 6$), 360 ($NPL = 12$), 528 ($NPL = 18$) and 696 ($NPL = 24$), and finally to 320 ($NPL = 8$), 608 ($NPL = 16$), 896 ($NPL = 24$) and 1184 ($NPL = 32$) for $d/a = 0.25$, 0.5, 0.75 and 1, respectively. The number of hydrodynamic panels along the width was 12 and 16 for the second and final group of idealizations, respectively. Table 2 shows the convergence of the predicted wet natural frequencies with increasing number of hydrodynamic panels for the first six wet modes. The differences between the results, based on the last two groups of idealizations, are reasonably small for all the submergence depths. Therefore, it may be said that the final group of idealizations (i.e., 320, 608, 896 and 1184 panel idealizations) adequately represents the distortional shapes of the partially submerged cantilever plate, and they were adopted for the calculations presented in Tables 3 and 4, and for those in Figs. 4 and 5. An additional convergence study was also carried out to establish the number of distortional modes needed for the predictions. As a result of this analysis, 12 in vacuo modes were included in the calculations.

3.2. Calculated results and comparisons

By solving the eigenvalue problem, Eq. (12), the uncoupled modes and associated frequencies of the cantilever plate of Lindholm et al. (1965), partially in contact with fluid, were obtained. The calculated natural frequencies are compared with the experimental measurements of Lindholm et al. (1965) in Table 3 for the plate oscillating in air (or in vacuo) or partially submerged in water (i.e., $d/a = 0.25$, 0.5, 0.75 and 1). Although, there are some differences between the predicted and measured results, the predicted wet natural frequencies show very good agreement with the corresponding experimental data. The differences lie in the range between 0.2% and 5.5%. For the same plate, Fig. 3 shows the in vacuo principal mode shapes (finite element results) whereas the calculated wet modes are presented in Fig. 4 for the depth ratio $d/a = 0.5$. The mode shapes shown in Figs. 3 and 4, corresponding to the first six wet (or dry) natural frequencies, are simply ordered with increasing frequency. As can be realized from the comparison of Fig. 4 with Fig. 3, the wet mode shapes vary slightly from the in vacuo modes. This is the hydrodynamic coupling of the in vacuo modes which creates negligible influence on the wet distortional mode shapes when the plate is partially submerged. Similar distortional mode shapes were also obtained for the depth ratios $d/a = 0{,}25$, 0.75 and 1, and therefore they are not presented here. It can also be observed from Table 3 that the frequencies behave as expected. That is to say the frequencies decrease with increasing area of contact with fluid. The largest area of contact was in the case of the fully submerged cantilever plate ($d/a = 1$). Therefore, the lowest frequencies occurred in this case (see Table 3).

Table 4 shows the calculated generalized added-mass terms for the depth ratios $d/a = 0.25$, 0.5, 0.75 and 1. The generalized added-mass terms in Table 4 are presented for the first 12 distortional in vacuo modes and they correspond

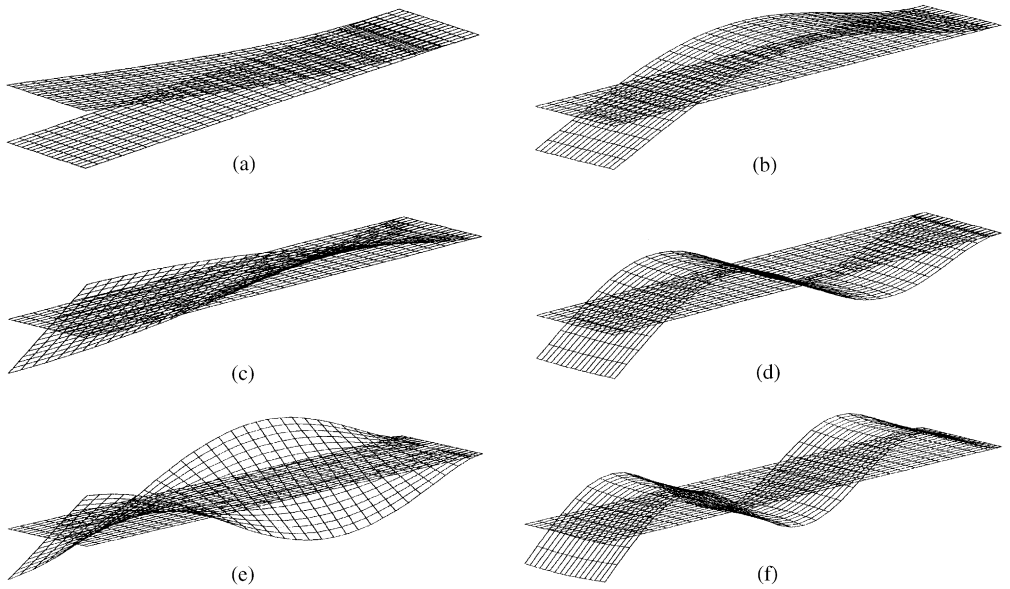

Fig. 3. In vacuo mode shapes of cantilever plate (FE results): (a) first mode, frequency 3.94 Hz; (b) second mode, frequency 24.66 Hz; (c) third mode, frequency 39.07 Hz; (d) fourth mode, frequency 69.24 Hz; (e) fifth mode, frequency 119.47 Hz; (f) sixth mode, frequency 136.35 Hz.

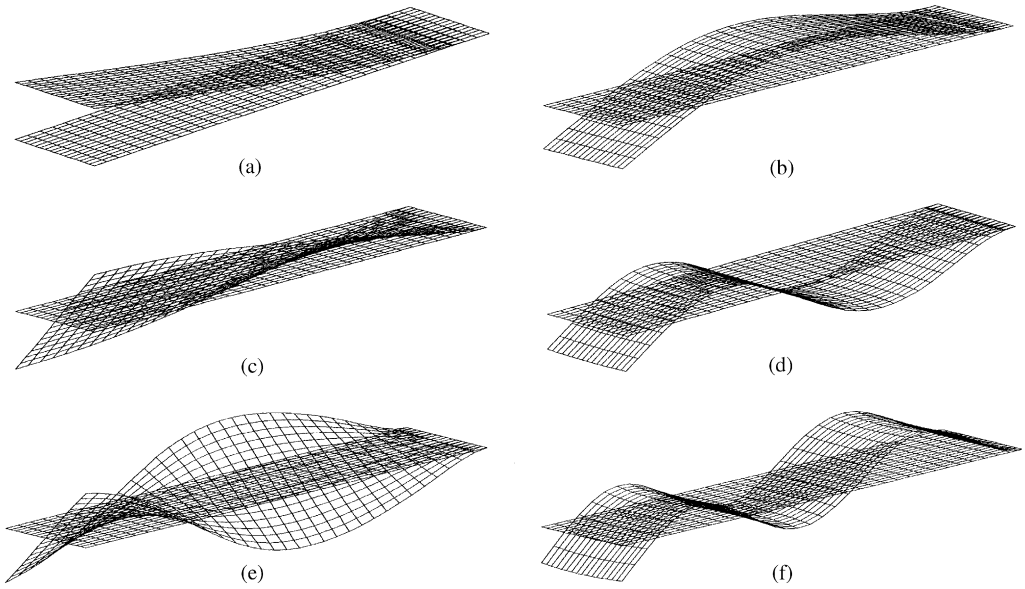

Fig. 4. Wet mode shapes of cantilever plate for depth ratio $d/a = 0.5$: (a) first mode, frequency 1.9 Hz; (b) second mode, frequency 15.69 Hz; (c) third mode, frequency 25.43 Hz; (d) fourth mode, frequency 52.23 Hz; (e) fifth mode, frequency 93.84 Hz; (f) sixth mode frequency 98.71 Hz.

to a generalized structural mass of $1\,\mathrm{kg\,m^2}$. Here, it is assumed that the structure preserves its in vacuo principal mode shapes in the fluid and that each mode gives rise to the surface pressure distribution of the flexible structure. However, the hydrodynamic forces associated with the inertial effect of the surrounding medium do not necessarily have the same spatial distribution as those of the in vacuo principal modes. Consequently this produces hydrodynamic coupling between the in vacuo modes. From Table 4, it is seen that the generalized added-mass matrices are symmetric and the

Table 4
Generalised added-mass coefficients (kg m^2) of partially submerged cantilever plate

		Mode	1	2	3	4	5	6	7	8	9	10	11	12
d/a	Mode	Mode type	S	S	A	S	A	S	S	A	S	A	S	A
0.25	1	S	1.956	1.034	−0.002	0.325	−0.001	−0.182	0.000	0.001	−0.411	0.003	−0.391	0.002
	2	S	1.034	0.693	0.000	0.400	0.000	0.152	0.000	0.000	−0.019	0.000	−0.109	0.000
	3	A	−0.002	0.000	0.738	0.000	0.587	0.000	0.000	0.333	0.000	0.064	0.000	−0.124
	4	S	0.325	0.400	0.000	0.428	0.000	0.383	0.000	−0.001	0.270	−0.001	0.115	−0.001
	5	A	−0.001	0.000	0.587	0.000	0.492	0.000	0.000	0.324	0.000	0.134	0.000	−0.017
	6	S	−0.182	0.152	0.000	0.383	0.000	0.498	0.000	−0.001	0.451	−0.002	0.286	−0.001
	7	S	0.000	0.000	0.000	0.000	0.000	0.000	0.005	0.000	0.000	0.000	0.000	0.000
	8	A	0.001	0.000	0.333	−0.001	0.324	−0.001	0.000	0.296	0.000	0.237	0.000	0.153
	9	S	−0.411	−0.019	0.000	0.270	0.000	0.451	0.000	0.000	0.485	−0.001	0.372	−0.001
	10	A	0.003	0.000	0.064	−0.001	0.134	−0.002	0.000	0.237	−0.001	0.313	0.000	0.307
	11	S	−0.391	−0.109	0.000	0.115	0.000	0.286	0.000	0.000	0.372	0.000	0.368	0.000
	12	A	0.002	0.000	−0.124	−0.001	−0.017	−0.001	0.000	0.153	−0.001	0.307	0.000	0.372
0.5	1	S	3.301	0.316	−0.001	−0.719	0.001	−0.440	0.000	0.001	0.023	−0.001	0.002	−0.001
	2	S	0.316	1.424	0.002	1.019	−0.002	−0.086	0.000	−0.001	−0.581	0.002	−0.213	0.001
	3	A	−0.001	0.002	1.349	0.000	0.472	0.000	0.000	−0.231	0.000	−0.193	0.000	0.071
	4	S	−0.719	1.019	0.000	1.337	−0.001	0.602	0.000	−0.001	−0.178	0.001	−0.324	0.000
	5	A	0.001	−0.002	0.472	−0.001	0.624	0.000	0.000	0.480	0.000	0.030	0.000	−0.214
	6	S	−0.440	−0.086	0.000	0.602	0.000	1.074	0.000	0.001	0.707	−0.001	−0.070	−0.001
	7	S	0.000	0.000	0.000	0.000	0.000	0.000	0.008	0.000	0.000	0.000	0.000	0.000
	8	A	0.001	−0.001	−0.231	−0.001	0.480	0.001	0.000	0.862	0.000	0.428	0.000	−0.125
	9	S	0.023	−0.581	0.000	−0.178	0.000	0.707	0.000	0.000	1.059	−0.001	0.524	0.000
	10	A	−0.001	0.002	−0.193	0.001	0.030	−0.001	0.000	0.428	−0.001	0.667	0.000	0.431
	11	S	0.002	−0.213	0.000	−0.324	0.000	−0.070	0.000	0.000	0.524	0.000	0.874	0.000
	12	A	−0.001	0.001	0.071	0.000	−0.214	−0.001	0.000	−0.125	0.000	0.431	0.000	0.721
0.75	1	S	3.660	−0.418	0.000	−0.447	0.001	−0.108	0.000	−0.001	−0.211	0.000	−0.079	0.000
	2	S	−0.418	3.117	0.001	0.149	−0.002	−0.702	0.000	0.002	0.106	−0.001	−0.213	0.000
	3	A	0.000	0.001	1.614	0.000	0.043	0.000	0.000	−0.165	0.000	0.063	0.000	−0.110
	4	S	−0.447	0.149	0.000	2.203	0.002	0.560	0.000	−0.002	−0.729	0.002	0.093	0.000
	5	A	0.001	−0.002	0.043	0.002	1.366	0.001	0.000	0.268	0.000	−0.337	0.000	0.158
	6	S	−0.108	−0.702	0.000	0.560	0.001	1.746	0.000	0.001	0.510	−0.001	−0.525	0.000
	7	S	0.000	0.000	0.000	0.000	0.000	0.000	0.008	0.000	0.000	0.000	0.000	0.000
	8	S	−0.001	0.002	−0.165	−0.002	0.268	0.001	0.000	1.126	0.000	0.354	0.000	−0.335
	9	S	−0.211	0.106	0.000	−0.729	0.000	0.510	0.000	0.000	1.603	0.000	0.355	0.000
	10	A	0.000	−0.001	0.063	0.002	−0.337	−0.001	0.000	0.354	0.000	1.045	0.000	0.289
	11	S	−0.079	−0.213	0.000	0.093	0.000	−0.525	0.000	0.000	0.355	0.000	1.453	0.000
	12	A	0.000	0.000	−0.110	0.000	0.158	0.000	0.000	−0.335	0.000	0.289	0.000	1.038
1	1	S	3.699	−0.534	0.000	−0.288	0.000	−0.242	0.000	0.000	−0.133	0.000	−0.103	0.000
	2	S	−0.534	3.515	0.000	−0.435	0.000	−0.176	0.000	0.000	−0.229	0.000	−0.085	0.000
	3	A	0.000	0.000	1.649	0.000	−0.050	0.000	0.000	−0.046	0.000	−0.046	0.000	−0.038
	4	S	−0.288	−0.435	0.000	3.134	0.000	−0.340	0.000	0.000	−0.097	0.000	−0.207	0.000
	5	A	0.000	0.000	−0.050	0.000	1.613	0.000	0.000	−0.051	0.000	−0.040	0.000	−0.046
	6	S	−0.242	−0.176	0.000	−0.340	0.000	2.719	0.000	0.000	−0.266	0.000	−0.060	0.000
	7	S	0.000	0.000	0.000	0.000	0.000	0.000	0.008	0.000	0.000	0.000	0.000	0.000
	8	A	0.000	0.000	−0.046	0.000	−0.051	0.000	0.000	1.549	0.000	−0.053	0.000	−0.035
	9	S	−0.133	−0.229	0.000	−0.097	0.000	−0.266	0.000	0.000	2.348	0.000	−0.213	0.000
	10	A	0.000	0.000	−0.046	0.000	−0.040	0.000	0.000	−0.053	0.000	1.466	0.000	−0.055
	11	S	−0.103	−0.085	0.000	−0.207	0.000	−0.060	0.000	0.000	−0.213	0.000	2.028	0.000
	12	A	0.000	0.000	−0.038	0.000	−0.046	0.000	0.000	−0.035	0.000	−0.055	0.000	1.371

cross-coupling terms are small in comparison with the diagonal ones. On the other hand, it can also be observed from Table 4 that the coupling effect generally becomes stronger for small submergence depths. For instance, the cross-coupling terms are mainly larger for the depth ratio, d/a, of 0.25 when compared with the fully submerged plate (depth ratio $d/a = 1$). Furthermore, it is also observed from Table 4 that there is negligibly small coupling between the symmetric (bending) and antisymmetric (torsional) modes.

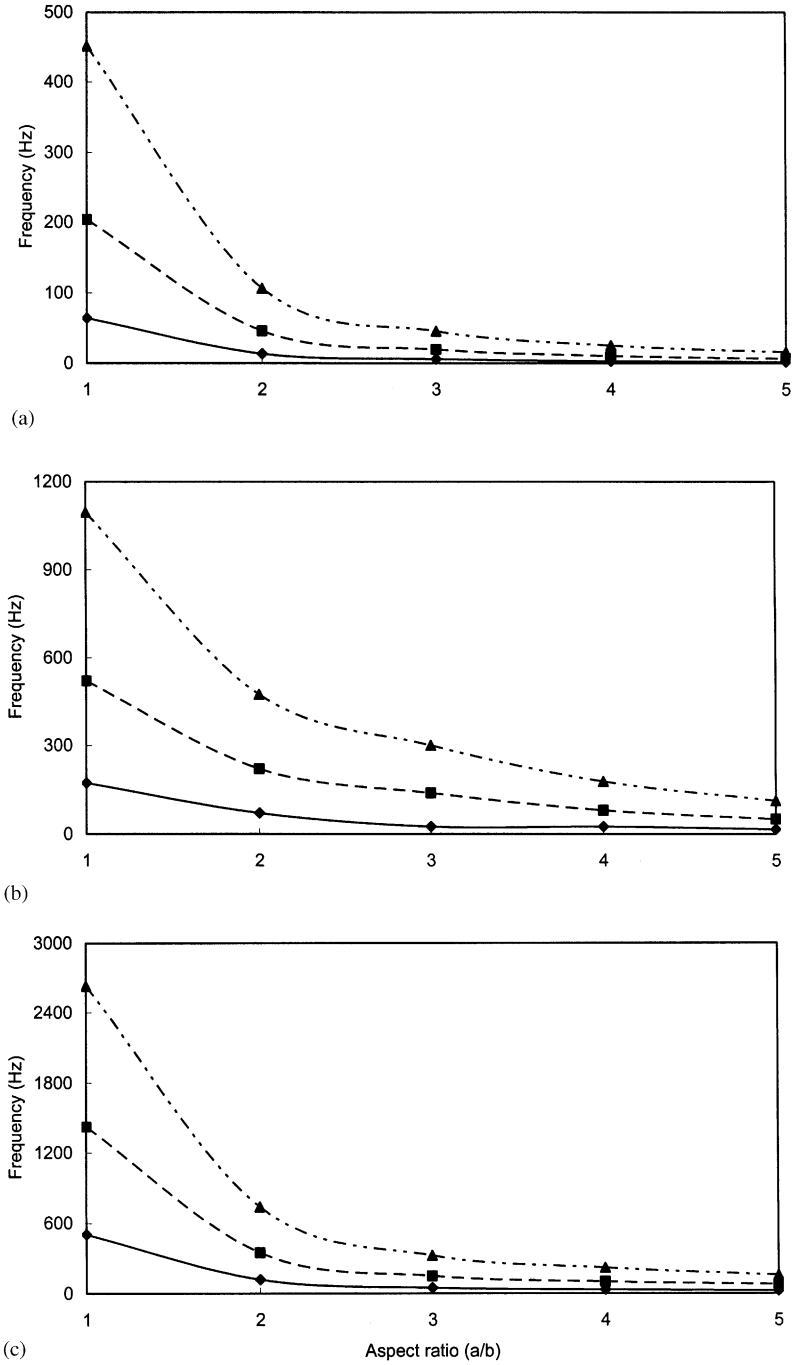

Fig. 5. Variation of wet frequencies with aspect ratio, a/b, and thickness ratio, t/b, for depth ratio $d/a = 0.5$: (a) first mode; (b) second mode; (c) third mode; (d) fourth mode; (e) fifth mode (f) sixth mode—, $t/b = 0.0238$;– – –, $t/b = 0.0611$;–· ·–· ·–,$t/b = 0.124$.

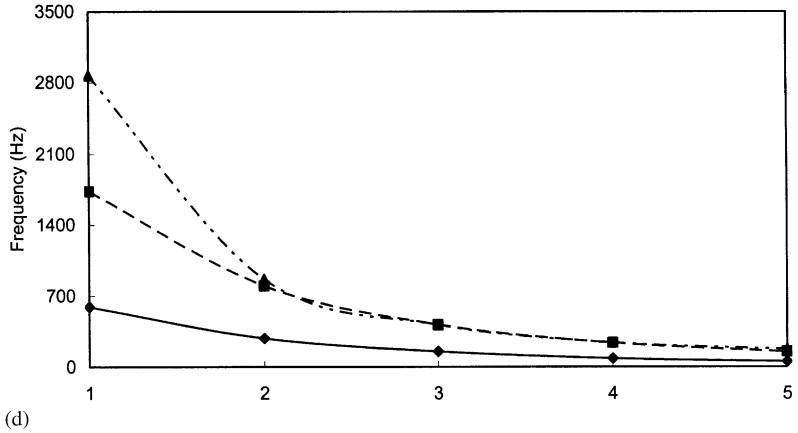

(d)

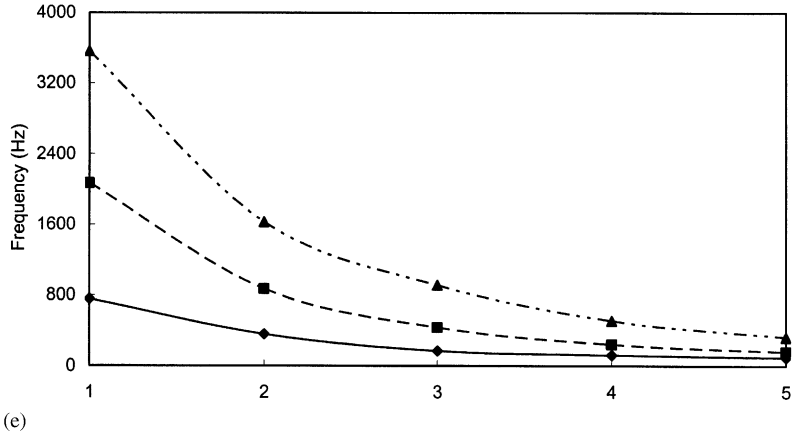

(e)

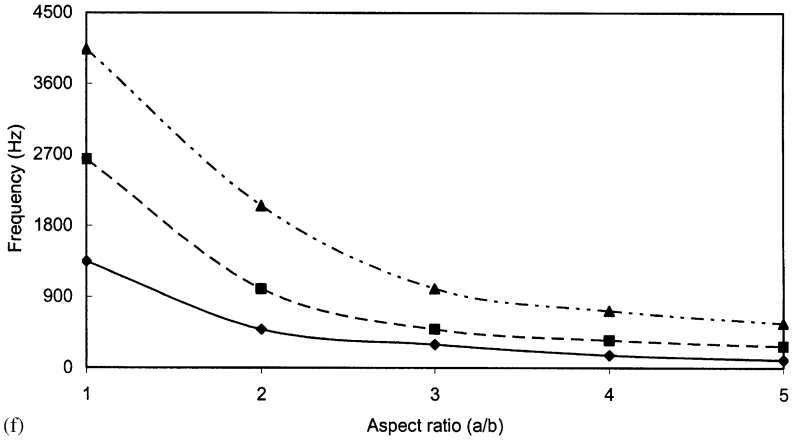

(f)

Fig. 5 (*continued*).

The analysis was subsequently extended to investigate the effects of plate aspect ratio, *a*/*b*, and thickness ratio, *t*/*b*, on the dynamic characteristics of this partially submerged cantilever plate. Fig. 5 shows the wet natural frequencies of the cantilever plate for three different thickness ratios, *t*/*b*, (i.e., 0.0238, 0.0611 and 0.124) and five different aspect ratios, *a*/*b*, (i.e., 1, 2, 3, 4 and 5), for the first six wet modes and depth ratio $d/a = 0.5$. As can be observed from Fig. 5, the wet natural frequencies decrease with increasing *a*/*b* values. However, they increase with increasing *t*/*b* values.

Table 5
Comparisons of dry and wet natural frequencies (Hz)

Mode	Mode type	This study					Fu and Price (1987)				
		In vacuo	Depth ratio (d/a)				In vacuo	Depth ratio (d/a)			
			0.25	0.5	0.75	1		0.25	0.5	0.75	1
1	S	2.04	1.58	1.30	1.20	1.17	2.06	1.63	1.31	1.21	1.17
2	A	4.98	4.09	3.51	3.31	3.28	5.05	4.20	3.48	3.26	3.22
3	S	12.48	11.46	10.23	8.60	8.00	12.70	11.66	10.41	8.70	8.03
4	S	15.82	13.66	12.06	11.22	11.07	16.10	13.86	12.20	11.38	11.21
5	A	18.04	16.61	15.37	13.21	12.58	18.40	16.81	15.62	13.25	12.55
6	S	31.23	29.08	27.39	23.96	22.98	—	—	—	—	—

In a further study, another cantilever plate, studied numerically by Fu and Price (1987), was adopted in the calculations. The in vacuo dynamic characteristics (i.e., natural frequencies and mode shapes) of the plate were obtained by using 256 finite elements (16 equally spaced elements along the length and width of the plate structure). The calculated natural frequencies are presented and compared with the predications of Fu and Price (1987) in Table 5. In their analysis, Fu and Price (1987) adopted 64 four-node thin plate elements (eight elements along the length and width of the plate). All the wet natural frequencies in Table 5 were evaluated by use of Eq. (12). The values of the current method compare well with those obtained from the theory adopted by Fu and Price (1987), as can be seen in Table 5. However, there are some differences between the results of the current method and those of Fu and Price (1987). The maximum difference is 4.5% and was observed for the depth ratio $d/a = 0.25$. For the converged results of the current method presented in Table 5, the wet surface of the cantilever plate is idealized by using 176, 320, 464, and 608 panels, respectively, for the depth ratios $d/a = 0.25$, 0.5, 0.75 and 1. The number of panels distributed along the length of the plate was 4, 8, 12, and 16, respectively, for the depth ratios $d/a = 0.25$, 0.50, 0.75 and 1. In all cases, 16 panels were distributed along the width of the plate. On the other hand, 12 in vacuo modes were adopted for the converged results of the current method presented in Table 5.

4. Conclusions

The dynamic characteristics (wet natural frequencies and associated modes) of two different, partially submerged cantilever plates were calculated by an approach based on the boundary-integral equation method and the method of images. It can be concluded from the results presented here that the method proposed is suitable for relatively high-frequency vibrations of partially submerged elastic structures.

From the results presented, the calculations based on the present method show very good agreement with the experimental data of Lindholm et al. (1965). The differences lie within the limits one would expect when comparing experimental data with numerical predictions. On the other hand, the results of the present method are also compared with the predictions of Fu and Price (1987) in Table 5, and there is good agreement between the two calculations. The predictions based on the current method are slightly lower in comparison with those of Fu and Price (1987).

As can be seen from Table 4, the generalized added-mass matrices are symmetric, and off-diagonal terms represent the effect of coupling between the in vacuo modes. It can also be concluded from Table 4 that the coupling becomes stronger with decreasing submergence depths.

It can also be concluded from the results in Tables 3 and 5 that the wet frequencies behave as expected from the theory. That is to say that the wet frequencies decrease with increasing submergence depth. Therefore, the lowest wet frequencies occur in the cases of fully submerged cantilever plates.

As can be seen from Fig. 5, the wet natural frequencies decrease with increasing aspect ratio, a/b, but increase with increasing thickness ratio, t/b.

The present study has demonstrated the versatility of the method through two different cantilever plates vibrating partially or fully submerged in water. In a future study, the effect of a flowing fluid on the dynamic characteristics of elastic structures will be considered.

Acknowledgements

This research was financially supported by Scientific and Technical Research Council of Turkey (Project No: ICTAG-1842). This support is gratefully acknowledged.

References

Amabili, M., Païdoussis, M.P., Lakis, A.A., 1998. Vibrations of partially filled cylindrical tanks with ring-stiffeners and flexible bottom. Journal of Sound and Vibration 213, 259–299.

ANSYS. 1994. User's Manual. ANSYS, Inc., Houston.

Bishop, R.E.D., Price, W.G., Wu, Y., 1986. A general linear hydroelasticity theory of floating structures moving in a seaway. Philosophical Transactions of the Royal Society of London A 316, 375–426.

Ergin, A., 1997a. The response behavior of a submerged cylindrical shells using the doubly asymptotic approximation method (DAA). Computers and Structures 62, 1025–1034.

Ergin, A., 1997b. An approximate method for the free vibration analysis of partially filled and submerged, horizontal cylindrical shells. Journal of Sound and Vibration 207, 761–767.

Ergin, A., 1997c. Dynamic characteristics of partially filled and submerged cylindrical tanks. Proceedings of the Eighth International Congress on Marine Technology, IMAM, Vol.**2,** Istanbul, pp 21–30.

Ergin, A., Price, W.G., Randall, R., Temarel, P., 1992. Dynamic characteristics of a submerged, flexible cylinder vibrating in finite water depths. Journal of Ship Research 36, 154–167.

Ergin, A., Temarel, P., 2002. Free vibration of a partially liquid-filled and submerged, horizontal cylindrical shell. Journal of Sound and Vibration 254, 951–965.

Fu, Y., Price, W.G., 1987. Interactions between a partially or totally immersed vibrating cantilever plate and the surrounding fluid. Journal of Sound and Vibration 118, 495–513.

Hess, J.L., 1975. Review of integral-equation techniques for solving potential-flow problems with emphasis on the surface-source method. Computer Methods in Applied Mechanics and Engineering 5, 145–196.

Hess, J.L., Smith, A.M.O., 1967. Calculation of potential flow about arbitrary bodies. Kuchemann, D., et al.,(Eds.), Progress in Aeronautical Sciences. Vol. 8, pp.1–138.

Kito, F., 1970. Principles of Hydro-elasticity. Keio University Publication, Tokyo.

Liang, C.-C., Liao, C.-C, Tai, Y.-S., Lai, W.-H., 2001. The free vibration analysis of submerged cantilever plates. Ocean Engineering 28, 1225–1245.

Lindholm, U.S, Kana, D.D., Chu, W.-H., Abramson, H.N, 1965. Elastic vibration characteristics of cantilever plates in water. Journal of Ship Research 9, 11–22.

Meyerhoff, W.K., 1970. Added masses of thin rectangular plates calculated from potential theory. Journal of Ship Research 14, 100–111.

Muthuveerappan, G., Ganesan, N., Veluswami, M.A., 1979. A note on vibration of a cantilever plate immersed in water. Journal of Sound and Vibration 63, 385–391.

Rao, P.S., Sinha, G., Mukhopadhyay, M., 1993. Vibration of submerged stiffened plates by the finite element method. International Shipbuilding Progress 40, 261–292.